ELSEVIER

Journal of Power Sources 75 (1998) 90–100

JOURNAL OF POWER SOURCES

Studies with porous zinc electrodes with additives for secondary alkaline batteries

R. Shivkumar, G. Paruthimal Kalaignan *, T. Vasudevan

Department of Industrial Chemistry, Alagappa University, Karaikudi— 630 003, Tamil Nadu, India

Received 15 September 1997; accepted 30 March 1998

Abstract

The effect of the presence of additives like ZnO, V_2O_5, PbO and $(NH_4)_2CS$ in solution phase on the performance of solid zinc electrode has already been reported. Small additions of HgO, Sb_2O_3, TiO_2 and Pb_3O_4 to the pasted zinc electrodes have been evaluated using Cyclic Voltammetry, Potentiodynamic Polarization (with temperature effect), A.C. Impedance measurements, Solution Analysis, and Porosity measurements. Though the additives HgO and Sb_2O_3 are known for their high hydrogen overpotential, HgO additive has the beneficial effect of imparting minimum standby corrosion, enhanced ageing behaviour and minimum shape change. As regards the additive TiO_2, its behaviour is superior to that of HgO as far as the ageing and high temperature performance are concerned. For Pb_3O_4, the corrosion behaviour as well as ageing are fairly good. However, this additive imparts a disadvantage of lead getting deposited on the counter electrode which would become a setback from the battery point of view. Details of the study are discussed in this paper. © 1998 Elsevier Science S.A. All rights reserved.

Keywords: Secondary alkaline batteries; Zinc electrodes; High hydrogen overpotential; Corrosion behaviour; Additives

1. Introduction

The zinc based batteries have high energy/power densities per unit volume when compared with other alkaline batteries. Although these batteries are commercially available, the problems of the zinc electrode like dendritic growth, shape change and high dissolution are not completely overcome. So far, many attempts have been undertaken to overcome these difficulties and still the problem remains elusive. Various additives like HgO [1], $Ca(OH)_2$ [2], Bi_2O_3 [3,4], Ga_2O_3 [5], Tl_2O_3 [6], $In(OH)_3$ [6,7], PbO [8,9], SnO_2 [9], etc., were added to the electrode to minimize these problems. A high cycle life alkaline zinc battery with inhibited dendritic or spongy zinc deposition with zinc anode containing SnO_2 and TiO_2 are reported [10]. Tsuji has reported about the stabilised discharge performance zinc anode having Titanium oxide (5%) of particle size 0.05 μ. The discharge capacity of the battery was around 80% for 200 charge–discharge cycles vs. 50 cycles at 80% for a battery with zinc anode containing 1% titanium oxide [11]. Zinc anodes for secondary alkaline batteries comprising of additives like PbO, SnO_2, Bi_2O_3, etc., that enhance the uniform distribution of the metal in the anode under charging conditions [12]. Jones evaluated that around 4 wt.% Pb_3O_4 and $Ca(OH)_2$ additives in zinc anodes reduce the tendency of the insoluble zincates toward cementation [13]. It can be stated that fundamental studies have been carried out to the least pin-pointing the cause of the failure and improvements the additives have made. In the present study, the above additives have been tried systematically to understand the basic mechanism of the dissolution of zinc and also the extent of standby corrosion the electrode would suffer in presence and absence of the additives. The logical aim of the study is to arrive at a suitable additive and optimize its composition so that the electrode has good ageing behaviour, minimum shape change, dendrite growth and standby corrosion with a view to fabricate a secondary zinc based alkaline system.

2. Experimental

2.1. Preparation of porous zinc electrodes

Pure zinc oxide powder of size 25–35 μm was mixed with Teflon emulsion and pressed onto a pure 40 grade

---

[*] Corresponding author

PII S0378-7753(98)00096-2

Nickel woven mesh of size 1 cm diameter and thickness of 0.15 mm. The thickness of the electrodes thus prepared were of 1.75 ± 0.2 mm. HgO, Sb_2O_3, TiO_2 and Pb_3O_4 additives were mixed separately with zinc oxide and the electrodes were prepared by the bulk mixing process. For each additive, four different compositions (HgO: 2.5–10.0%, Sb_2O_3: 2–8%, TiO_2: 1–4%, Pb_3O_4: 0.5–2.0%) were tried. The prepared electrodes were reduced at the potential of −1800 mV vs. Hg/HgO electrode in 6 M KOH and the experiments were performed.

2.2. Solution analysis

To assess the standby corrosion of the electrode, solution analysis was undertaken. The electrode was dipped into 50 ml of 6 M KOH solution taken in a beaker. After 3 h, the electrode was removed. To 10 ml of the solution, glacial acetic acid was added till the pH drops approximately to 8. Then a slight excess of 5% 8-hydroxy quinoline was added till the precipitation was complete. The precipitate obtained was filtered using a weighed sintered G-4 crucible, washed with hot water to remove the excess of reagent, dried at 110°C and weighed. Duplicate was also carried out to confirm the results.

2.3. Potentiodynamic polarization

A three electrode cell assembly was used [14,15] with a Hg/HgO electrode as the reference electrode, a platinum foil as the counter electrode and the porous zinc electrode as the working electrode. Polarization experiments were performed using a Potentiostat, coupled with a scan generator and recorder over the range of −1650 mV to −1200 mV in 6 M KOH solution at a constant scan rate of 1 mV s^{-1}. The effects of temperature on the polarization were also determined for the additives at their maximum protecting compositions.

2.4. A.C. impedance technique

Impedance measurements were carried out using PAR model 6310. As the system includes a micro computer with a dedicated software, it is possible to merge the data from Lock-in and FFT (Fast Fourier Transform) measurements and display the impedance data over a wide range of frequencies. The cell assembly used was the same as in polarization technique. The working electrode was dipped in the electrolyte for about 5–10 min to attain a steady state open circuit potential. The frequency range applied was between 100 mHz to 10 kHz and the amplitude of A.C. signal was 10 mV. Nyquist plots were used to interpret the results.

2.5. Cyclic voltammetry

The zinc electrodes were kept at −1800 mV vs. Hg/HgO for 5 min in 6 M KOH solution, disconnected, shaken to free-off adsorbed hydrogen bubbles and polarized from −2300 to −300 mV at different sweep rates (1–2.5 mV s^{-1}). The potential was fixed after several experiments to get reproducible E–i curves for different sweep rates. The experiments were performed for each composition of the additives for 1st, 8th and 15th days to assess the ageing behaviour of the electrodes.

2.6. Porosity measurements

The porosity of the electrodes were 80 to 95% and determined by the Xylene impregnation method. The weighed (A g) zinc electrode was kept in xylene below 30 mm mercuric pressure for 1 h in a vacuum flask. The electrode was removed and weighed in air (B g) and in water (C g). The percentage of porosity is given by:

$$P = \frac{100(B-A)d_w}{(B-C)d_x}$$

where d_w = density of water; d_x = density of xylene.

3. Results and discussions

3.1. Solution analysis

Solution analysis for the zinc contents dissolved were carried out in 6 M KOH and the results are presented in Table 1. It is found that the electrode containing lower composition of HgO (2.5%) gives the minimum dissolution. As the concentration of HgO content increases, the dissolution rate of the electrode also increases. This could be attributed to the HgO forming a separate phase of noble character. In the case of Sb_2O_3, for all compositions, there

Table 1
Corrosion studies of porous zinc electrodes with and without additives through solution analysis data

Composition of the electrode	Weight loss (g)	Percentage inhibition
Reduced ZnO (B)	0.0592	–
B + 2.5% HgO	0.0235	60.30
B + 5.0% HgO	0.0310	47.64
B + 7.5% HgO	0.0436	26.35
B + 10.0% HgO	0.0583	1.52
B + 2% Sb_2O_3	0.0821	*38.68
B + 4% Sb_2O_3	0.0963	*62.67
B + 6% Sb_2O_3	0.1073	*81.25
B + 8% Sb_2O_3	0.1364	*130.41
B + 1% TiO_2	0.0968	*63.51
B + 2% TiO_2	0.0853	*44.09
B + 3% TiO_2	0.0745	*25.84
B + 4% TiO_2	0.0622	*5.07
B + 0.5% Pb_3O_4	0.0261	55.91
B + 1.0% Pb_3O_4	0.0392	33.78
B + 1.5% Pb_3O_4	0.0516	12.84
B + 2.0% Pb_3O_4	0.0984	*66.22

*Stimulation.

Table 2
Potentiodynamic polarization of porous zinc electrodes with and without additives of different compositions in 6 M KOH; scan rate 1 mV s^{-1}

Composition of the electrode	OCP (mV)	E_{corr} (mV)	i_{corr} (mA)	Tafel slope (mV/decade)		At $E_{corr}+100$ mV (mA)		% Reduction of partial currents	
				b_a	b_c	i_a	i_c	i_a	i_c
Reduced ZnO (B)	−1453	−1439	0.6210	76	202	7.279	2.043	–	–
B + 2.5% HgO	−1432	−1399	0.1888	55	200	4.894	0.530	32.77	74.06
B + 5.0% HgO	−1467	−1459	0.2462	56	234	5.484	0.496	24.66	75.72
B + 7.5% HgO	−1448	−1444	0.4521	65	155	6.210	1.887	14.69	7.64
B + 10.0% HgO	−1461	−1458	0.6062	100	245	4.962	1.350	35.54	33.92
B + 2% Sb_2O_3	−1435	−1413	1.0000	86	135	7.880	3.857	*8.26	*88.79
B + 4% Sb_2O_3	−1436	−1412	1.8880	127	187	10.830	5.736	*48.78	*180.76
B + 6% Sb_2O_3	−1425	−1403	2.0430	136	182	9.237	6.210	*26.90	*203.96
B + 8% Sb_2O_3	−1417	−1390	3.0390	188	251	10.830	8.532	*48.78	*317.62
B + 1% TiO_2	−1425	−1410	1.3740	113	108	7.880	9.237	*8.26	*352.13
B + 2% TiO_2	−1415	−1395	1.0000	62	76	6.700	9.047	7.95	*342.83
B + 3% TiO_2	−1425	−1412	0.9745	69	60	9.237	7.279	*26.90	*256.29
B + 4% TiO_2	−1418	−1400	0.7881	53	50	10.000	8.532	*37.38	*317.62
B + 0.5% Pb_3O_4	−1457	−1453	0.1833	83	211	2.336	0.695	67.91	65.98
B + 1.0% Pb_3O_4	−1417	−1410	0.3675	79	292	4.489	0.741	38.33	63.73
B + 1.5% Pb_3O_4	−1458	−1449	0.5484	90	192	5.484	1.402	24.66	31.38
B + 2.0% Pb_3O_4	−1410	−1404	1.1720	84	89	7.279	2.019	0	1.17

*Stimulation.

Table 3
Potentiodynamic polarization of porous zinc electrodes with and without additives in 6 M KOH at different temperatures; scan rate = 1 mV s^{-1}

Composition of the electrode	Temperature (K)	OCP (mV)	E_{corr} (mV)	i_{corr} (mA)	Tafel slope (mV/decade)		At E_{corr} + 100 mV (mA)		Percent reduction		E_{act} (kJ mol^{-1} K^{-1})	Adsorption energies with additives (kJ mol^{-1} K^{-1})
					b_a	b_c	i_a	i_c	i_a	i_c		
Reduced ZnO (blank)	303	−1453	−1439	0.6210	76	202	7.279	2.043	–	–	−47.868	–
	308	−1448	−1431	0.6700	87	207	6.062	1.823	–	–		
	313	−1448	−1434	0.7280	158	229	3.039	1.374	–	–		
	318	−1440	−1431	1.2688	161	321	4.520	1.743	–	–		
	323	−1430	−1412	1.7434	210	253	5.298	4.175	–	–		
	328	−1436	−1428	2.3556	186	277	3.889	2.728	–	–		
Blank + 2.5% HgO	303	−1432	−1399	0.1888	55	200	4.894	0.530	32.76	74.05	−67.813	−19.945
	308	−1434	−1426	0.5223	67	79	6.236	4.924	∗2.87	∗170.10		
	313	−1430	−1424	0.6615	89	53	5.878	2.728	∗93.42	∗98.54		
	318	−1447	−1434	0.9047	110	218	6.062	2.228	∗34.12	∗27.83		
	323	−1449	−1436	1.2688	107	232	6.210	2.395	∗17.21	49.20		
	328	−1433	−1424	1.4873	166	339	5.298	2.218	∗36.23	18.70		
Blank + 2% Sb_2O_3	303	−1435	−1413	1.0000	86	135	7.880	3.857	∗8.26	∗88.79	−33.188	+14.680
	308	−1419	−1394	1.1722	74	87	10.000	8.532	∗64.96	∗368.02		
	313	−1429	−1405	1.3737	115	158	7.880	5.796	∗159.30	∗321.83		
	318	−1418	−1396	1.7434	120	195	9.237	5.736	∗104.36	∗229.09		
	323	−1407	−1381	2.0431	174	198	7.279	6.210	∗37.39	∗ 48.74		
	328	−1407	−1383	2.5930	158	174	10.000	9.237	∗157.14	∗238.60		
Blank + 4% TiO_2	303	−1418	−1400	0.7881	53	50	10.000	8.532	∗37.38	∗317.62	−28.721	+19.147
	308	−1444	−1427	0.8531	124	284	4.520	1.610	25.44	11.68		
	313	−1451	−1422	0.9428	158	300	3.888	1.701	∗ 27.94	∗23.80		
	318	−1430	−1412	1.2688	124	158	7.279	5.298	∗ 61.04	∗203.96		
	323	−1440	−1419	1.5118	192	237	4.642	3.455	12.38	26.72		
	328	−1438	−1416	1.7434	152	228	7.279	4.175	∗87.17	∗53.04		
Blank + 0.5% Pb_3O_4	303	−1457	−1453	0.1888	63	211	2.336	0.695	67.91	65.98	−49.783	−1.915
	308	−1446	−1433	0.3582	70	208	4.175	1.172	31.13	35.71		
	313	−1454	−1438	0.4062	81	250	4.962	0.819	∗63.28	40.39		
	318	−1442	−1426	0.5736	82	174	5.736	2.043	∗26.90	∗17.21		
	323	−1441	−1429	0.7406	100	229	6.062	1.650	∗14.42	65.01		
	328	−1439	−1431	0.9047	113	242	6.700	1.823	∗72.28	33.17		

∗Stimulation.

is only stimulation of corrosion. This could be explained as due to the low oxygen over-voltage of the Sb_2O_3 phase. With regards to TiO_2, as the composition is increased from 1 to 4%, the dissolution of zinc is decreased. But in all compositions, TiO_2 additive has resulted in enhanced dissolution of zinc, which is similar to that of Sb_2O_3. In the case of Pb_3O_4, it is found that low composition of 0.5 and 1.0% are most effective in reducing the corrosion of zinc. Even the composition of 1.5% gives a slight protection, whereas 2.0% additive composition causes nearly 66% stimulation of corrosion. As regards the contrasting effect of Pb_3O_4 at higher composition, it can be stated that the additive at lower composition acts as an impurity and increases the over-voltage of the cathodic reaction. However, at higher composition, it is possible that the additive could form a more noble separate phase leading to higher corrosion of zinc.

3.2. Potentiodynamic polarization

The Tafel parameters of the additives at room temperature and at different temperatures are presented in Tables 2 and 3 and Fig. 1. In the case of HgO additive, as in the solution analysis results, there is slightly enhanced dissolution at 10% HgO composition. The OCP values, except for 2.5% HgO, have shown a slight cathodic shift and so is the case with E_{corr} values. At all compositions, b_c is greater than b_a, indicating that the reaction is mostly under cathodic control. This is also evident from the percentage reduction of partial currents i_a and i_c at $E_{corr} \pm 100$ mV [16]. From the studies, it may be concluded that 2.5% HgO composition would be most suited from the standby corrosion point of view. As regards the additive Sb_2O_3, it is found that all compositions stimulate corrosion. The OCP and E_{corr} values have shown gradual shift in the positive direction and the percentage stimulation of anodic partial current is comparatively lower. All these indicate that the electrode reaction is under anodic control. In the case of TiO_2 the OCP has shown a slight positive shift of about 30 mV. There is stimulation of partial currents at $E_{corr} \pm 100$ mV and the stimulation is less for anodic than for cathodic implying the reaction to be under anodic control. The additive Pb_3O_4 also shows a positive shift in OCP and E_{corr} values with increased composition. However, the

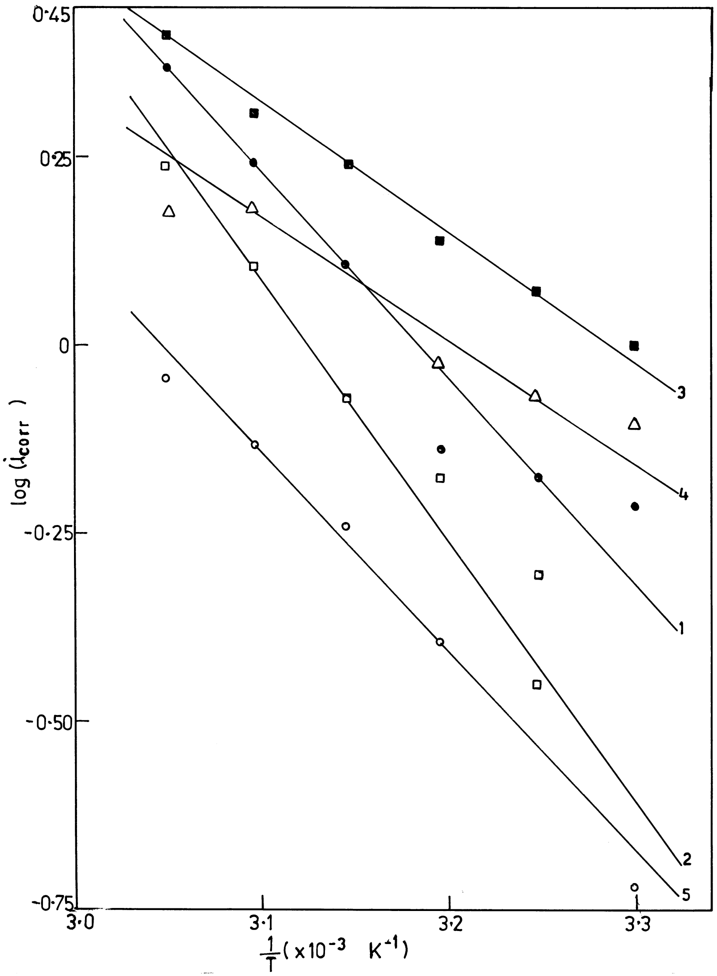

Fig. 1. Effect of temperature on the corrosion of porous zinc electrode with and without additives in 6 M KOH (from polarization results). (1) Reduced ZnO (B); (2) B + 2.5% HgO; (3) B + 2% Sb_2O_3; (4) B + 4% TiO_2; (5) B + 0.5% Pb_3O_4.

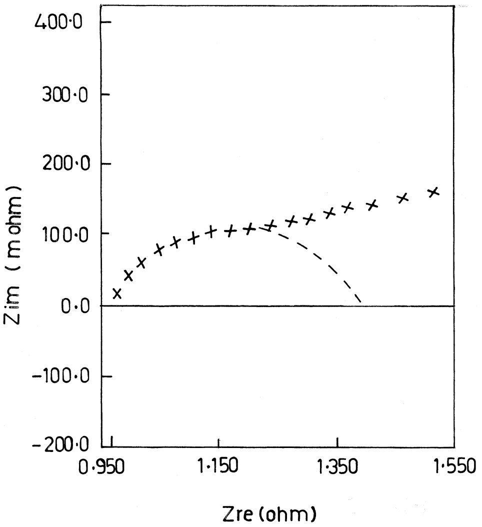

Fig. 2. Nyquistian diagram for porous zinc electrode in 6 M KOH.

reduction in cathodic partial currents are more pronounced than that of the anodic ones implying its cathodic nature.

In the case of HgO and Pb_3O_4 additives, the change in the activation energy for the dissolution reaction of the electrodes are in the more negative direction indicating the more exothermic nature of the additives. It is also evident from nearly 8- and 5-fold increase in their respective corrosion currents over the temperature range of 303–328 K. But in the case of Sb_2O_3 and TiO_2 additives, the activation energy of the reactions shift in the more positive direction indicating their endothermic nature with only about 2.5-fold increase in their i_{corr} values between the same temperature range.

3.3. A.C. impedance technique

Figs. 2–4 represent the Nyquist diagrams for the blank, 2.5% HgO and 4% TiO_2 additives, respectively. The anodic behaviour of zinc through impedance technique has been reported [17]. Some mechanistic information can be obtained from the shape of the impedance diagram [18]. The absence of any inductive loops suggest that the system is a simple corroding system. The R_t and capacity values are presented in Table 4. The R_t values reflect the trend in behaviour of the additives. The lower capacity values indicate less charge in interface accounting for reduced dissolution. In the case of 2.5% HgO, where there is minimum dissolution, the rising portion of the impedance plot indicates the reaction to be under diffusion control. For 4% TiO_2, there are two semi-circles, may be one corresponding to the oxidation of zinc and the other to the dissolution of the oxidised product. Such types of impedance plots are reported for Hg/propylene carbonate + NaI/β alumina/propylene carbonate + NaI/Hg cell at 295 K which are explained due to the difference in conductivity of the two processes taking place in the cell [19].

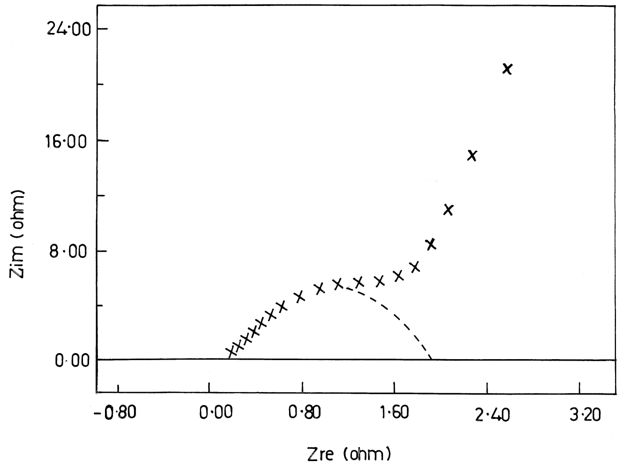

Fig. 3. Nyquistian diagram for porous zinc electrode containing 2.5% HgO in 6 M KOH.

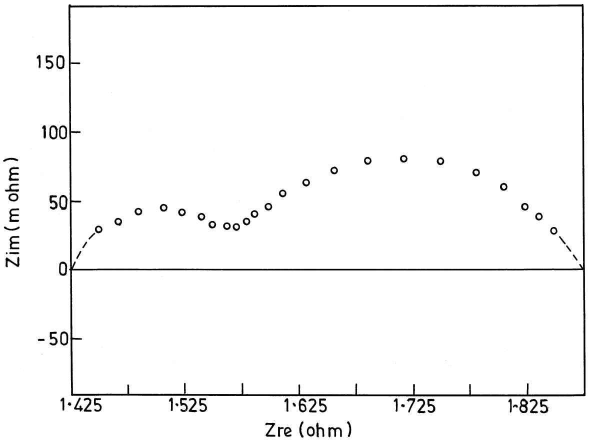

Fig. 4. Nyquist diagram for porous zinc electrode containing 4% TiO_2 in 6 M KOH.

3.4. Cyclic voltammetry

Fig. 5 shows a typical cyclic voltammogram of porous zinc electrode in 6 M KOH at a scan rate of 1 mV s^{-1}. The shape of the voltammogram is similar to that of the

Table 4
Parameters derived from Impedance measurements for porous zinc electrodes with and without additives in 6 M KOH

Electrode composition	f_{max} (Hz)	R_t (Ω)	C_{dl} (F cm^{-1})
Reduced ZnO (B)	398.1	0.463	8.648×10^{-4}
B + 2.5% HgO	158.5	1.831	5.487×10^{-4}
B + 10.0% HgO	398.10	0.491	8.146×10^{-4}
B + 2% Sb_2O_3	63.10	0.241	1.047×10^{-2}
B + 8% Sb_2O_3	39.81	0.056	7.143×10^{-2}
B + 1% TiO_2	631.0	0.130	1.941×10^{-3}
B + 4% TiO_2	398.1	0.450	8.889×10^{-4}
B + 0.5% Pb_3O_4	158.5	1.675	5.998×10^{-4}
B + 2.0% Pb_3O_4	631.0	0.110	2.294×10^{-3}

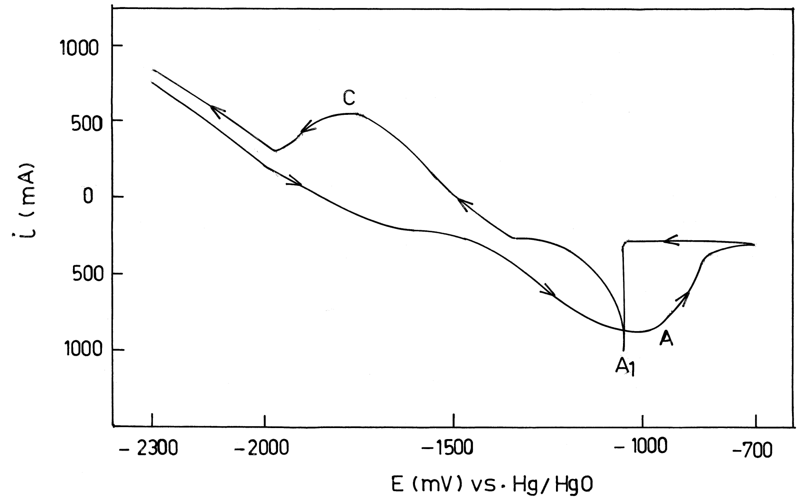

Fig. 5. Typical cyclic voltammogram of porous zinc electrode in 6 M KOH at a scan rate of 1 mV s^{-1}.

solid electrode cited by Farr and Hampson [20,21] and also confirmed in the earlier works [22] except that of high current flow due to large surface area. The basic mechanism of the electrode reaction could be the same as for the solid electrode which is as follows.

$$Zn_{kink} \rightarrow Zn_{ad} \tag{1}$$

$$Zn_{ad} + 2OH^{-} \rightarrow Zn(OH)^{2-}_{2\,ad} \tag{2}$$

$$Zn(OH)^{2-}_{2\,ad} \rightarrow Zn(OH)_{2\,ad} + 2e^{-} \tag{3}$$

$$Zn(OH)_{2\,ad} \rightarrow Zn(OH)_{2\,diss} \tag{4}$$

$$Zn(OH)_{2\,diss} + 2OH^{-} \rightarrow Zn(OH)^{2-}_{4} \tag{5}$$

On increasing the scan rate, the anodic peaks A and A_1 move in the anodic direction, while C in the cathodic direction. This indicates that the value of ΔE_p increases with scan rate and the peak currents of all the peaks A, A_1, and C also increase. As the scan number increases, the ΔE_p values decreases. This indicates the better reversibility of the electrode. On the 8th day of ageing behaviour of the electrode, the peak A_1 disappears due to the saturation of the solution with zincate. The peak currents of both A and C are drastically decreased. On further ageing, no peak is observed in both directions due to the failure of the electrode.

In the case of HgO additive, at lower composition (2.5%), during the reverse scan two more anodic peaks A_2 and A_3 have appeared (Fig. 6). This is due to the possibility of following dissolution mechanism.

$$Zn + 2OH^{-} \rightarrow ZnO + H_2O + 2e^{-} \tag{6}$$

$$ZnO + H_2O \rightarrow [Zn(OH)_2]_{ad} \tag{7}$$

$$[Zn(OH)_2]_{ad} + 2OH^{-} \rightarrow [Zn(OH)_4]^{2-}_{ad} \tag{8}$$

$$[Zn(OH)_4]^{2-}_{ad} \rightarrow [Zn(OH)_4]^{2-}_{diss} \tag{9}$$

The first step corresponds to the oxidation of zinc to zinc oxide resulting in peak A. In this step, where the current increases with scan rate, is due to the particular step not being limited in current in the range of scan rates used. The peak A_1 is due to the formation of $[Zn(OH)_2]_{ad}$ species. There is a reverse trend in i_p values corresponding to the third step indicating that this step leading to the chemical dissolution is slow. As the scan rate increases, the peaks A, A_1 and A_3 shift in the positive and A_2 and C in the negative directions. As in the case of blank, the ΔE_p values increase with scan rate due to the decrease in reversibility of the electrode. On the 8th day, the peak A_3 disappears (Table 5) due to the saturation of the solution with zincate. It is noted that the peak A_2 is also a part of oxidation. There is cathodic shift with scan rate due to the requirement of enhanced energy for the dissolution process on the 1st day. However, at the end of 8th day, the trend is opposite due to the process requiring lower energy. Again

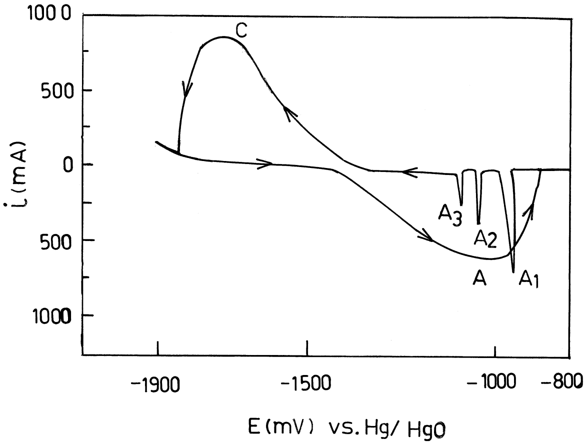

Fig. 6. Typical cyclic voltammogram of porous zinc electrode containing 2.5% HgO in 6 M KOH (scan rate 1 mV s^{-1}).

Table 5
Parameters derived from cyclic voltammetry for the ageing behaviour of 2.5% HgO additive in 6 M KOH

Number of days	Scan rate (mV s^{-1})	Peak potential (mV)					Peak current (mA)					ΔE_p (mV)
		A	A_1	A_2	A_3	C	A	A_1	A_2	A_3	C	
1	1.0	−1010	−955	−1044	−1102	−1756	631	700	376	249	854	746
	1.5	−937	−935	−1055	−1096	−1826	754	797	360	395	1057	889
	2.0	−912	−858	−1065	−1063	−1897	918	897	350	476	1181	985
	2.5	−817	−812	−1078	–	−2187	1148	1069	342	–	1322	1370
8	1.0	−1090	−1034	−1070	–	−1604	190	125	70	–	215	514
	1.5	−1039	−988	−1067	–	−1675	254	235	85	–	304	636
	2.0	−982	−980	−1064	–	−1746	310	270	90	–	402	764
	2.5	−896	−970	–	–	−1844	356	276	–	–	520	948
15	1.0	−1328	–	–	–	−1372	18	–	–	–	20	44
	1.5	−1292	–	–	–	−1426	31	–	–	–	36	134
	2.0	−1286	–	–	–	−1480	49	–	–	–	73	194
	2.5	−1238	–	–	–	−1496	79	–	–	–	89	258

Table 6
Parameters derived from cyclic voltammetry for porous zinc electrode with various compositions of HgO in 6 M KOH

Composition of the electrode	Scan rate (mV s^{-1})	Peak potential (mV)					Peak current (mA)					ΔE_p (mV)	Q_a/Q_c
		A	A_1	A_2	A_3	C	A	A_1	A_2	A_3	C		
Blank + 2.5% HgO	1.0	−1010	−955	−1044	−1102	−1756	631	700	376	249	854	746	0.858
	1.5	−937	−935	−1055	−1096	−1826	754	797	360	395	1057	889	0.960
	2.0	−912	−858	−1065	−1063	−1897	918	897	350	476	1181	985	0.986
	2.5	−817	−812	−1078	–	−2168	1148	1069	342	–	1322	1317	1.112
Blank + 5.0% HgO	1.0	−980	−1025	–	–	−1823	631	487	–	–	836	843	0.852
	1.5	−882	−993	–	–	−1956	777	650	–	–	1003	1074	0.930
	2.0	−830	−985	–	–	−2003	890	723	–	–	1250	1173	0.965
	2.5	−798	−980	–	–	−2148	1107	786	–	–	1442	1350	1.008
Blank + 7.5% HgO	1.0	−982	−1074	–	–	−1804	−468	−431	–	–	603	812	0.673
	1.5	−926	−1028	–	–	−1876	−783	−696	–	–	1054	950	0.755
	2.0	−850	−983	–	–	−1953	−896	−787	–	–	1230	1103	0.836
	2.5	−682	−908	–	–	−2138	−1347	−1036			1601	1456	1.210
Blank + 10.0% HgO	1.0	−1025	−941	–	–	−1730	658	667	–	–	750	705	0.847
	1.5	−938	−921	–	–	−1877	777	763	–	–	930	939	0.922
	2.0	−840	−895	–	–	−1982	928	906	–	–	1198	1142	1.123
	2.5	−662	−870	–	–	−2005	1167	968	–	–	1402	1343	1.293

Table 7
Parameters derived from cyclic voltammetry for porous zinc electrode with various compositions of Sb_2O_3 in 6 M KOH

Composition of the electrode	Scan rate (mV s^{-1})	Peak potential (mV)			Peak current (mA)		
		A	A_1	C	A	A_1	C
Blank + 2% Sb_2O_3	1.0	−931	−1033	−1828	323	335	482
	1.5	−824	−1023	−1897	497	423	738
	2.0	−768	−996	−1963	703	476	993
	2.5	−603	−963	–	1012	514	–
Blank + 4% Sb_2O_3	1.0	−1057	−1038	−1672	243	298	316
	1.5	−908	−1030	−1836	338	367	471
	2.0	−867	−1016	−1902	438	466	741
	2.5	−702	−905	–	1048	506	–
Blank + 6% Sb_2O_3	1.0	−1012	−1023	−1763	268	317	376
	1.5	−987	−1018	−1976	468	447	621
	2.0	−864	−1012	–	631	467	–
	2.5	−618	−728	–	996	881	–
Blank + 8% Sb_2O_3	1.0	−946	−1022	−1803	391	429	587
	1.5	−867	−1010	–	527	471	–
	2.0	−754	−996	–	628	496	–
	2.5	−738	−971	–	883	512	–

Table 8
Parameters derived from cyclic voltammetry for porous zinc electrode with various compositions of TiO_2 in 6 M KOH

Composition of the electrode	Scan rate (mV s^{-1})	Peak potential (mV)					Peak current (mA)				
		A	A_1	A_2	A_3	C	A	A_1	A_2	A_3	C
Blank + 1.0% TiO_2	1.0	−904	−912	−1006	−1039	−1860	442	698	402	298	737
	1.5	−759	−885	−952	−1015	−1974	657	760	550	409	870
	2.0	−703	−834	−933	−997	−2002	783	787	625	421	993
	2.5	−694	−792	−880	−952	−2147	878	897	660	457	1168
Blank + 2.0% TiO_2	1.0	−1022	−1026	–	–	−1707	651	654	–	–	968
	1.5	−964	−1018	–	–	−1808	823	849	–	–	1178
	2.0	−916	−1009	–	–	−1881	868	931	–	–	1476
	2.5	−798	−1004	–	–	−1997	1327	1436	–	–	1704
Blank + 3.0% TiO_2	1.0	−1035	−1003	–	–	−1741	499	823	–	–	880
	1.5	−977	−992	–	–	−1816	819	1013	–	–	1065
	2.0	−913	−988	–	–	−1910	929	1048	–	–	1243
	2.5	−792	−958	–	–	−2052	1135	1063	–	–	1458
Blank + 4.0% TiO_2	1.0	−1018	−933	–	–	−1739	577	830	–	–	787
	1.5	−945	−896	–	–	−1824	685	898	–	–	937
	2.0	−873	−865	–	–	−1913	822	915	–	–	1097
	2.5	−782	−735	–	–	−2053	1127	1470	–	–	1127

this is confirmed by the increased current with scan rate during 8th day. The ageing behaviour holds good till the 15th day and then the electrode loses its capacity. But in the case of higher composition of HgO, no extra peaks are observed (Table 6) and the mechanism followed seems to be that of blank. For 10% HgO composition, the electrode failure occurs after the 8th day itself.

In the case of Sb_2O_3, the same mechanism as for the blank is followed. As the scan rate is increased to 2.5 mV s^{-1}, no cathodic peak is observed which indicates the poor charging behaviour of the electrode. As the composition of Sb_2O_3 increases, the reduction peak C vanishes even at lower scan rates due to the irreversible character imparted by Sb_2O_3 (Table 7). On using this additive, the electrode failure occurs even after the 1st day. Also these electrodes undergo shape change which is visibly observed by the bulging of the electrode after a few cycles. This could be due to the Sb_2O_3 particles decreasing the nucleation rate and increasing the growth rate for zinc deposition. This defect is not observed in the case of HgO.

The results of the additive TiO_2 corresponding to various compositions and scan rates are presented in Table 8. The pattern of the voltammogram for 1% TiO_2 additive is similar to that of 2.5% HgO additive with A, A_1, A_2 and A_3 anodic peaks and one cathodic peak C. The scheme of the anodic dissolution process is the same as for HgO. But from the trends in the shift of the peaks and current values, it is inferred that the rate controlling step is different. In the case of TiO_2 unlike HgO, A_2 has shown an anodic shift. As regards the current values, again A_2 shows a different trend, i.e., the current increases with scan rate. However, the rate of increase is the least for A_1, i.e., only

Table 9
Parameters derived from cyclic voltammetry for the ageing behaviour of 3% TiO_2 additive in 6 M KOH

Number of days	Scan rate (mV s^{-1})	Peak potential (mV)			Peak current (mA)			ΔE_p (mV)
		A	A_1	C	A	A_1	C	
1	1.0	−1035	−1003	−1741	499	823	880	706
	1.5	−977	−992	−1816	819	1013	1065	839
	2.0	−913	−988	−1910	929	1048	1243	997
	2.5	−792	−958	−2052	1135	1063	1458	1260
8	1.0	−1077	−1013	−1742	308	440	412	665
	1.5	−1038	−1005	−1780	379	496	513	742
	2.0	−953	−998	−1802	577	560	640	849
	2.5	−882	−978	−1896	583	571	790	1014
15	1.0	−1138	−1041	−1615	217	370	359	477
	1.5	−1108	−1037	−1664	258	386	368	556
	2.0	−1053	−1024	−1731	293	390	622	678
	2.5	−976	−998	−1879	351	410	662	903

Table 10
Parameters derived from cyclic voltammetry for porous zinc electrode with various compositions of Pb_3O_4 in 6 M KOH

Composition of the electrode	Scan rate (mV s^{-1})	Peak potential (mV)					Peak current (mA)				
		A	A_1	A_2	A_3	C	A	A_1	A_2	A_3	C
Blank + 0.5% Pb_3O_4	1.0	−1002	−895	−1016	−1069	−1773	270	318	307	144	359
	1.5	−922	−814	−1018	−1071	−1884	356	510	300	131	457
	2.0	−796	−810	−1023	−1074	−2058	488	576	298	120	646
	2.5	−487	−798	−1039	−1080	−2302	681	608	250	107	878
Blank + 1.0% Pb_3O_4	1.0	−932	−773	−982	−1058	−1893	727	1008	698	286	972
	1.5	−827	−765	−993	−1065	−2014	931	1198	663	275	1248
	2.0	−782	−764	−1008	−1072	−2058	1087	1261	631	225	1336
	2.5	−638	−760	−1016	−1085	−2108	1361	1341	588	174	1406
Blank + 1.5% Pb_3O_4	1.0	−941	−788	−996	−1048	−1815	718	1027	723	390	923
	1.5	−856	−769	−1002	−1055	−1896	827	1148	650	314	1151
	2.0	−792	−758	−1005	−1059	−1975	978	1267	642	250	1316
	2.5	−708	−751	−1027	−1071	−2060	1224	1304	523	183	1492
Blank + 2.% Pb_3O_4	1.0	−879	−768	−981	−1030	−1913	675	912	567	230	943
	1.5	−773	−735	−992	−1040	−2023	852	1023	558	228	1088
	2.0	−733	−728	−997	−1046	−2133	971	1125	552	198	1278
	2.5	−612	−716	−1002	−1055	−2212	1075	1163	548	193	1414

25% as against nearly 50% for A, A_2 and A_3. This could lead to the inference that the reaction of ZnO to $[Zn(OH)_2]_{ad}$ is slower corresponding to the peak A_1. The patterns for 2%, 3%, and 4% TiO_2 additives are similar to that of the blank with the absence of A_2 and A_3 peaks. From ageing point of view, it is found that the higher composition of TiO_2 additive is beneficial, evident from increased i_p values for both anodic and cathodic peaks. The results of the ageing behaviour of 3% TiO_2 is presented in Table 9.

Table 10 represents the results obtained for different compositions of Pb_3O_4 additive corresponding to various scan rates. The behaviour of the additive is similar to that of 1% TiO_2 suggesting that the dissolution mechanism is the same as in the earlier case. However, it is to be noted that as the scan rate increases, the peaks A_2 and A_3 shift in the negative direction while the currents show decreasing trend. The rate of decrease in current is more for A_3. Hence, it could be explained that the dissolution of $[Zn(OH)_4]^{2-}_{ad}$ is the slowest step. Table 11 represents the results for the ageing behaviour of 1.5% Pb_3O_4 additive. This additive has almost the same performance as that of TiO_2 as for as the ageing behaviour is concerned. Also this material is cheaper than TiO_2. In spite of this advantage and good ageing behaviour, its usage as an electrode additive is not preferred due to the fact that during cycling, it is unmistakably noted that lead gets deposited at the counter electrode. From the battery point of view, this would cause a severe setback as it could lead to poisoning of the positive electrode. The $(\Delta E_p)_{v=0}$ and $(Q_a/Q_c)_{v=0}$ values are presented in Table 12. By considering these values, the electrode of 2.5% HgO and 3% TiO_2 composi-

Table 11
Parameters derived from cyclic voltammetry for the ageing behaviour of 1.5% Pb_3O_4 additive in 6 M KOH

Number of days	Scan rate (mV s^{-1})	Peak potential (mV)				Peak current (mA)						ΔE_p (mV)
		A	A_1	A_2	A_3	C	A	A_1	A_2	A_3	C	
1	1.0	−941	−788	−996	−1048	−1815	718	1027	723	390	923	874
	1.5	−856	−769	−1002	−1055	−1896	827	1148	650	314	1151	1030
	2.0	−792	−758	−1005	−1059	−1975	978	1267	642	250	1316	1183
	2.5	−708	−751	−1027	−1071	−2060	1224	1304	523	183	1492	1352
8	1.0	−965	−835	−961	−1015	−1796	381	530	327	227	783	831
	1.5	−888	−829	−1006	−1057	−1852	587	674	351	197	898	964
	2.0	−767	−788	−1019	−1066	−1965	596	825	442	177	1023	1198
	2.5	−729	−770	−1015	−1074	−2028	727	873	512	142	1113	1299
15	1.0	−1026	−877	−989	−1037	−1717	200	270	167	159	296	691
	1.5	−991	−865	−992	−1052	−1756	260	374	194	156	377	765
	2.0	−947	−815	−995	−1068	−1804	307	380	279	146	434	857
	2.5	−917	−805	−998	−1077	−1866	359	402	290	138	492	1049

Table 12
Effect of various composition of additives in porous zinc electrode in 6 M KOH on the reversibility of charge–storage reaction

Composition of the electrode	$(\Delta E_p)_{v=0}$ (mV)	$(Q_a/Q_c)_{v=0}$
Reduced ZnO (B)	365	0.596
B + 2.5% HgO	455	0.688
B + 5.0% HgO	515	0.740
B + 7.5% HgO	505	0.528
B + 10.0% HgO	530	0.568
B + 1% TiO_2	650	0.560
B + 2% TiO_2	345	0.450
B + 3% TiO_2	325	0.600
B + 4% TiO_2	405	0.505
B + 0.5% Pb_3O_4	390	0.605
B + 1.0% Pb_3O_4	650	0.465
B + 1.5% Pb_3O_4	370	0.660
B + 2.0% Pb_3O_4	600	0.580

tions are having better reversibility and hence most suitable for electrode fabrication.

4. Conclusions

Among the different additives tried, lower compositions of HgO and Pb_3O_4 are the better additives from the standby corrosion point of view. From polarization studies, the cathodic nature of HgO and Pb_3O_4 and anodic character of Sb_2O_3 and TiO_2 are evident. TiO_2 and Sb_2O_3 will be the better additives for high temperature performance of the electrode due to their endothermic character of the electrode reaction. The charge transfer resistance values obtained from impedance studies also confirm the solution analysis results. The ageing behaviour of the electrodes obtained from cyclic voltammetry studies indicate that lower composition of HgO and an optimum compositions of TiO_2 and Pb_3O_4 will be most suited from battery point of view. However, Pb_3O_4 is not encouraged as it could lead to poisoning of the other electrode. Also, Sb_2O_3 causes bulging and shape changes after a few cycles. From the studies, 2.5% HgO and 3% TiO_2 additives are recommended for electrode preparation to have stability and good ageing behaviour.

5. List of symbols

OCP	Open circuit potential
E_{corr}	Corrosion potential
i_{corr}	Corrosion current
b_a and b_c	Anodic and cathodic Tafel slopes
i_a and i_c	Anodic and cathodic partial currents
E_{act}	Energy of activation
f_{max}	Maximum frequency
R_t	Charge transfer resistance
C_{dl}	Double layer capacitance
i_p	Peak current
E_p	Peak potential
(ΔE_p)	Peak potential separation
Q_a and Q_c	Anodic and cathodic peak charges
$(\Delta E_p)_{v=0}$	Peak potential separation at zero scan rate
$(Q_a/Q_c)_{v=0}$	Ratio of anodic and cathodic peak charges at zero scan rate

Acknowledgements

One of the authors, R. SHIVKUMAR, SRF, gracefully acknowledges CSIR, New Delhi, for their award of fellowship to carry out this piece of work.

References

[1] Jerome Goodkin, U.S. Pat. 3, 493, 434 (1970).
[2] S. Sekido, T. Ohhira, T. Yogoyama, Y. Ikeda, Jpn. Kokai 75, 09, 725 (1975).
[3] K. Aizawa, Y. Shirogami, H. Yosushi, T. Takamura, Jpn. Kokai Tokkyo Koho 78, 73, 332 (1978).
[4] J. McBreen, E. Gannon, J. Power Sources 15 (1985) 169.
[5] L. Yu Gun'ka, N.G. Nikhalenko, V.N. Flerov, Zh. Prikl. Khim. 54 (1981) 77.
[6] Sanehiro Furukawa, Shuzo Murakami, Jpn. Kokai Tokkyo Koho JP 60, 185, 373 (1985).
[7] Sanehiro Furukawa, Mitsuzo Nogami, Mikiaki Todokora, Jpn. Kokai Tokkyo Koho JP 03, 122, 235 (1991).
[8] Kazuya Okabe, Yoshihiro Eguchi, Toshiyaki Astuda, Kankichi Fujii, Jpn. Kokai Tokkyo Koho JP 04, 126, 356 (1992).
[9] J. McBreen, E. Gannon, Electrochim. Acta 26 (1981) 1439.
[10] Sanyo Electric Company, Jpn. Kokai Tokkyo Koho 58, 163, 162 (1983).
[11] H. Tsuji, Jpn. Kokai Tokkyo Koho 79, 122, 838 (1979).
[12] S. Furukawa, M. Nogami, M. Todokora, Jpn. Kokai Tokkyo Koho, JP 03, 046, 759 (1991).
[13] R.A. Jones, Eur. Pat. 28, 879 (1981).
[14] S. Barnatt, J. Electrochem. Soc. 39 (1952) 549.
[15] M. Prazak, Werkst. Korros. 25 (1974) 104.
[16] T. Vasudevan, S. Alwarappan, S. Muralidharan, S. Venkatakrishna Iyer, Corr. Sci. 37 (1995) 1235.
[17] R.D. Amstrong, M.F. Bell, J. Electroanal. Chem. 55 (1974) 201.
[18] H. Schweickert, W.J. Lorenz, H. Friedburg, J. Electrochem. Soc. 127 (1980) 1693.
[19] R.D. Amstrong, D.P. Sellick, J. Appl. Electrochem. 9 (1979) 623.
[20] J.P.G. Farr, N.A. Hampson, Trans. Faraday Soc. 62 (1996) 3493.
[21] J.P.G. Farr, N.A. Hampson, J. Electroanal. Chem. 13 (1967) 433.
[22] R. Shivkumar, G. Paruthimal Kalaignan, T. Vasudevan, J. Power Sources 55 (1995) 53.